



## **BIOFIDELIC DESIGN OF THE FOREARM OF A MYOELECTRIC PROSTHESIS WITH MAXIMUM FUNCTIONAL VOLUME**

**Ramananarivo, Mathieu; Raison, Maxime; Barron, Olivier; Achiche, Sofiane**  
École Polytechnique de Montréal, Canada

### **Abstract**

The congenital or traumatic amputation of upper limbs leads to strong mobility and socio-psychological disabilities. The amputees can choose between three types of prostheses: cosmetic, body-powered and myoelectric. The myoelectric prostheses are controlled via electromyographic activity, they provide control over more degrees of freedom. The development of myoelectric prostheses is largely influenced by breakthroughs in robotics, sensors and machine learning technologies. As a consequence, the development of upper-limb prostheses is mainly technology driven without taking into account the low user acceptance. To improve the biofidelity of existing prostheses, a biomimetic approach has been explored by the work presented here. In this paper we propose an alternative biofidelic mechanism developed to be used in an operational prosthesis. The main results are the production of a mechanism optimized to reproduce with a low and controlled error of the pronation-supination movement while using a single actuator. The mechanism solid shapes are designed to be usable in an operational prosthesis.

**Keywords:** Biomedical design, Bio-inspired design / biomimetics, 3D printing, Design to X, Prostheses

### **Contact:**

Mathieu Ramananarivo  
École Polytechnique de Montréal  
Mechanical Engineering  
Canada  
mathieu.ramananarivo@polymtl.ca

Please cite this paper as:  
Surnames, Initials: *Title of paper*. In: Proceedings of the 21<sup>st</sup> International Conference on Engineering Design (ICED17),  
Vol. 1: Resource-Sensitive Design | Design Research Applications and Case Studies, Vancouver, Canada, 21.-25.08.2017.

## 1 INTRODUCTION

The upper limbs are of the utmost importance for carrying daily tasks. The congenital or traumatic amputation of upper limbs leads to strong mobility and socio-psychological disabilities. There are generally three main categories of prostheses available for amputees: cosmetic, body-powered and myoelectric. The cosmetic prostheses are passive, they are a good imitation of the healthy limb and give the amputee the comfort of a "normal" natural look but they are not convenient for practical tasks. The body-powered devices are actuated with straps attached to the patient's back, they are handy for simple tasks but usually only enable the control of a single degree of freedom. The myoelectric prostheses are controlled via electromyographic (EMG) activity, they provide control over more degrees of freedom with a greater strength than the body-powered devices. The development of myoelectric prostheses is largely influenced by breakthroughs in robotics, sensors and machine learning technologies. As a consequence, the development of upper-limb prostheses is mainly technology driven without taking into account the low user acceptance (Peerdeman et al., 2011). A study (Otto et al., 2015) shows that full use of prostheses was attained in only 48% of the above elbow amputee. The main reason for this low-acceptance is the difference between the technical solutions available on the market and the needs of the amputees. Cosmetic prostheses are not practical, body-powered ones are less adapted for complex tasks and lack a natural appearance (Biddiss, et al., 2007). While myoelectric prostheses also look unnatural, they remain expensive and their control interface is generally not intuitive and requests a lot of training for the amputee to gain minimal control over the prostheses (Cipriani et al., 2008).

To improve the biofidelity of existing prostheses, a biomimetic approach has been explored by researchers. Herr et al. have developed a biofidelic forearm mechanism. This mechanism uses the parallel structure of the bones to reproduce the natural pronation supination movement. This approach enables individuals suffering from limb amputation to more readily accept their new artificial appendages as part of their own body, rather than foreign objects that must simply be tolerated (Herr et al., 2003). In this paper we propose an alternative biofidelic mechanism developed to be used in an operational prosthesis. It is worth noting that this work is part of a larger design project of our research group to develop a smart and biofidelic myoelectric prosthesis for trans-humeral amputees.

## 2 DEFINITION AND OPTIMIZATION OF THE MECHANISM

Most of the prostheses that allow for pronation-supination movements use a pivot joint usually placed at the end (wrist) of the artificial forearm. This provokes a discontinuity in the rotation that is not present in the human forearm: there is no separation between the hand and the forearm. As shown in Figure 1. This rotation is achieved by crossing the radius and the ulna (McFarlane, 2010) and therefore achieving natural pronation and supination.

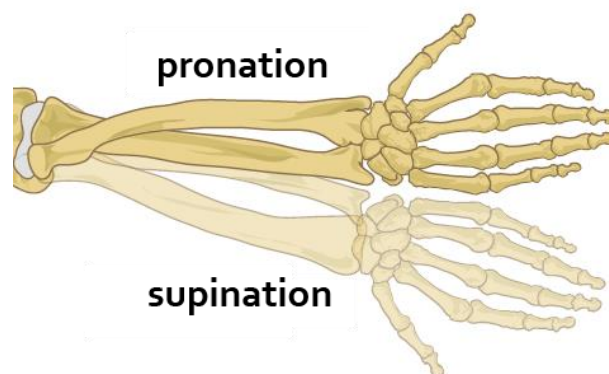


Figure 1. Pronation and supination movements adapted from (Laitenberger et al., 2015)

### 2.1 Kinematic modeling of the forearm

The human upper limb is composed of three parts, the arm, the forearm and the hand. The kinematic chain of the upper limb that reproduces the skeleton structure is presented in (**Error! Reference source not found.**). The arm is modeled by one solid that extends from the shoulder to the elbow and

corresponds to the humerus. The forearm is represented by a parallel mechanism involving two solids: the radius and the ulna. The study, presented by our research group (Laitenberger et al., 2015), provided a very accurate forearm model, the joints choices resulted from the motion capture and analysis of the pronation-and supination movement of several patients. This bio-accurate kinematic model is close to the one found in (Herr et al., 2003), as both use the pronation-supination axis (PS axis) extending from the approximate center of the proximal head of the radius (HR) to the distal head of the ulna (RU) (**Error! Reference source not found.**). This definition is known as the reference but in the context of the prosthesis design, it has the disadvantage of presenting divergence between the average position of the forearm axis and the PS axis. In other words, the pronation-supination rotation is carried out around the little finger instead of being around the middle finger. In this paper; we use another definition where the PS axis extends from the approximate center of the elbow to the approximate center of the wrist (Kapandji, 1982). Even though this definition is less biomechanically accurate it allows us to avoid the divergence problem cited above. Also, it is to be noted that the model presented in **Error! Reference source not found.** requires two different actuators when the pronation-supination movement represents one single degree of freedom. The new adopted definition allows us to also solve this over-actuation problem. Therefore; the new biomechanical model, developed in this paper, is illustrated in Figure 3.

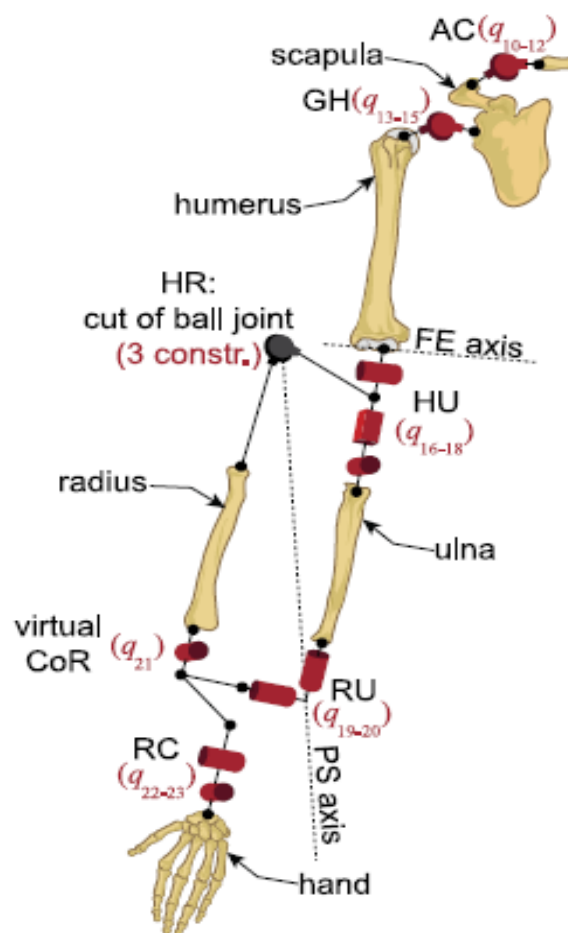


Figure 2. Kinematic chain of the upper limb. The model is articulated by the acromioclavicular joint (AC,  $q_{10-12}$ ), the glenohumeral joint (GH,  $q_{13-15}$ ), the humeroulnar joint (HU,  $q_{16-18}$ ), the radioulnar joint (RU,  $q_{19-20}$ ), the virtual CoR ( $q_{21}$ ), the humeroradial joint (HR, cut of ball joint with three kinematic loop-closure constraints), and the radiocarpal joint (RC,  $q_{22-23}$ ) adapted from (Laitenberger et al., 2015)

## 2.2 Definition of the proposed mechanism

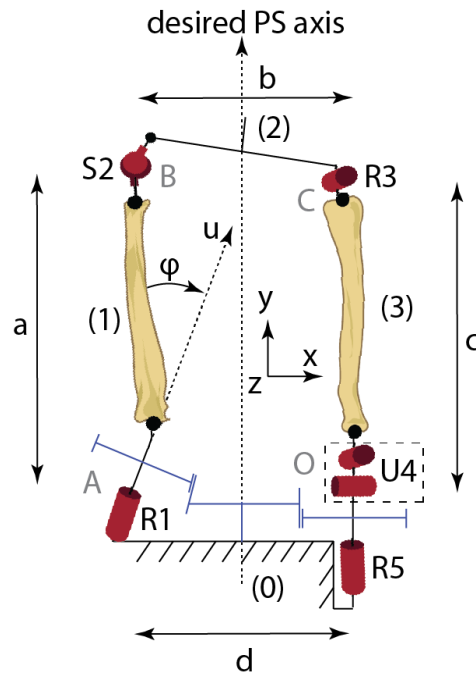


Figure 3. Kinematic chain of the proposed forearm mechanism. elbow (0), ulna (1), hand (2), radius (3). Gear system (blue). Mechanism dimensions:  $a = c = 200\text{mm}$  and  $d = b = 50\text{mm}$

As cited above, the kinematic model developed, in this paper, for the prosthesis is illustrated in Figure 3. The elbow (0), ulna (1), hand (2) and radius (3) are represented. R1 and R5 joints have their control law paired by a gear system, visible in Figure 3, and are actuated by a single motor. The characteristics of each joint are specified in Table 1.

Table 1. Joints characteristics

JOINTS	CHARACTERISTICS
<b>PIVOT R1</b>	(A, u)
<b>SPHERICAL S2</b>	(B)
<b>PIVOT R3</b>	(C, z)
<b>UNIVERSAL U4</b>	(x, z, O)
<b>PIVOT R5</b>	(y, D)

It is worth noting that our new proposed mechanism has a design shortcoming at the gears level. As seen in Figure 3, the axis of the three gears are not parallel. In other words, the middle gear is spur gear on the right, and bevel gear on the left which is a problem for the physical implementation. This was solved by using a gap between the left gears.

All joints have their axis defined by one of the Cartesian axis except the R1 joint which rotates around the  $u$  axis. The  $u$  axis is obtained by rotating around the  $y$  axis with the angle  $\varphi$  (Figure 3). This angle has to be optimized so that the pronation-supination axis (PS axis) of the proposed mechanism is the same as the one defined in Section 2.1, i.e. the average axis extending from the center of the elbow to the center of the wrist as shown in (Figure 3). It is worth noting, that the mechanism is not planar and represents a major improvement on the previous model developed in our research group.

### 2.2.1 Geometric closing

The elbow (0) is considered as the base and  $O$  the origin. Therefore the coordinates of point A are :

$$A = \begin{bmatrix} -d \\ 0 \\ 0 \end{bmatrix} \quad (1)$$

B is rotating around  $u$  with the angle  $\gamma_1$ . Hence his coordinates are :

$$B = \begin{bmatrix} -d + a * \sin(\varphi) * \cos(\varphi) * (\cos(\gamma_1) - 1) \\ a * \sin(\varphi)^2 * \cos(\gamma_1) + a * \cos(\varphi)^2 \\ a * \sin(\varphi) * \sin(\gamma_1) \end{bmatrix} \quad (2)$$

As U4 and R5 axis are intersecting at the same point O, they could have been merged into one spherical joint. The reason the articulation is composed of both a pivot and a universal joint is that one of the rotations is actuated (R5,  $\gamma_5$ ) and the remaining two are passive joints (U4).

O and B are spherical equivalent joints. If R1 is blocked, the plan  $\mathcal{P}_{OBC}$  defined by the points O, B and C will rotate around OB axis. As the universal joint is not homokinetic, the rotation speed  $\omega_2$  of  $\mathcal{P}_{OBC}$  is given by (Equation 3). For a universal joint, if  $\theta$  is defined as the angle between the input axis (y) and output axis (OC):

$$\frac{\omega_2}{\gamma_4} = \frac{\cos(\theta)(1+\tan^2(\gamma_5))}{1+\cos^2(\theta)\tan^2(\gamma_5)} \quad (3)$$

The oscillation amplitude of the input speed over the output is given by:

$$err(\%) = \frac{1}{\cos(\theta)} - \cos(\theta) \quad (4)$$

The proposed mechanism only allows very small values for  $\theta$ , the error from homokineticity is less than 5%. Thus it is possible to approximate with a controlled error the rotation of plan OBC:  $\omega_{OBC} = \gamma_5$ .

$C_{OBC}$  is defined as the coordinates of the point C given in  $\{x_3, y_3, z_3\}$   $\mathcal{P}_{OBC}$  axis system. In this frame:

$$C_{OBC} = \begin{bmatrix} c * \sin(\alpha_3) * \cos(\gamma_5) \\ c * \cos(\alpha_3) \\ c * \sin(\alpha_3) * \sin(\gamma_5) \end{bmatrix} \quad (5)$$

The coordinates  $\{x_3, y_3, z_3\}$  are obtained after two consecutive rotation around x and z axes with respectively the angles  $\theta_1$  and  $\theta_2$ .  $y_3$  axis is aligned with OB.

To obtain the coordinate in the reference axis system  $\{x, y, z\}$ , two rotations ( $Rot_1$  &  $Rot_2$ ) needs to be applied:

$$Rot_1 = \begin{bmatrix} 1 & 0 & 0 \\ 0 & \cos(\theta_1) & \sin(\theta_1) \\ 0 & -\sin(\theta_1) & \cos(\theta_1) \end{bmatrix} \quad (6)$$

$$Rot_2 = \begin{bmatrix} \cos(\theta_2) & \sin(\theta_2) & 0 \\ -\sin(\theta_2) & \cos(\theta_2) & 0 \\ 0 & 0 & 1 \end{bmatrix} \quad (7)$$

where:

$$\tan(\theta_1) = \frac{z_B}{y_B} \text{ et } \tan(\theta_2) = \frac{x_B}{y_B} \quad (8)$$

$$C = Rot_1 * Rot_2 * C_{OBC} \quad (9)$$

The last unknown angle  $\alpha_3$  can be calculated from the other known lengths in OBC triangle.

$$\cos(\alpha_3) = \frac{\|OB\|^2 + c^2 - b^2}{2 * \|OB\| * c} \quad (10)$$

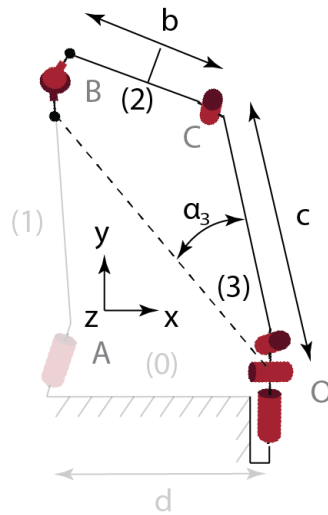


Figure 4. Representation of  $\alpha_3$

### 2.3 Optimization of the angle $\varphi$

The goal of this section is to find the optimal value for  $\varphi$  that minimizes the average distance  $D_m$ .  $D_m$  is the average value of the distances between the center of the wrist/hand (Solid 2 in Figure 3 and 4) and the desired PS-axis during a full pronation-supination movement ( $180^\circ$ ). The actuated joints are R1 and R5, their control laws are paired via a gear system ( $\gamma_1 = \gamma_5$ ) with  $\gamma_1 \in [-90^\circ; 90^\circ]$ . This gear system can be seen (Figure 3 and the right side of Figure 6).

The direct kinematic previously calculated is implemented and the movement is discretized with a step  $p_{\gamma_1} = 1^\circ$ . For each movement step the distance  $d_{PSaxis}$  between the center of the wrist and the desired PS axis is calculated. The mean distance  $D_m$  is then obtained. This criteria is calculated for  $\varphi \in [0^\circ; 20^\circ]$  with  $p_\varphi = 0.1^\circ$ . It is worth noting that the optimization of the mechanism is performed using MATLAB (MATHWORKS, USA).

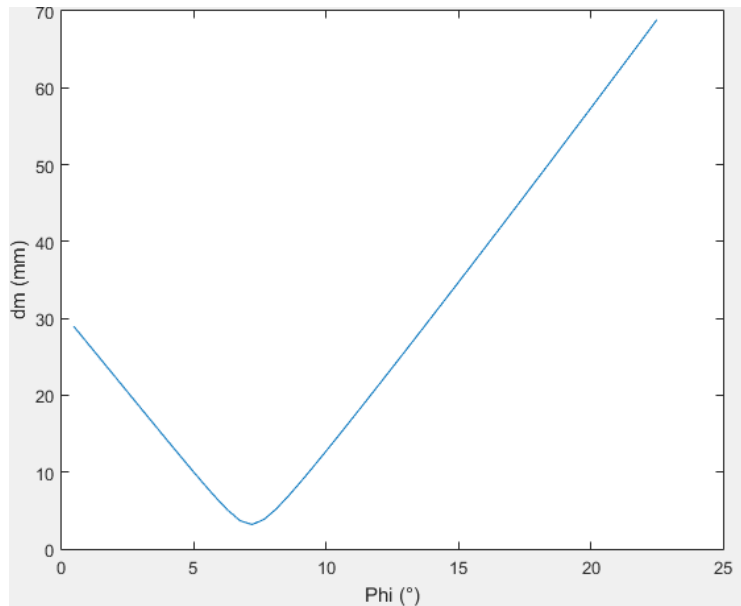


Figure 5.  $D_m$  minimization graph :  $\varphi(D_m)$

As shown in the graph, the optimal angle  $\varphi = 7.0^\circ$  gives a mean distance  $D_m = 4.5\text{mm}$ . This is the closest this mechanism can get from the desired pronation-supination axis to achieve a natural movement.

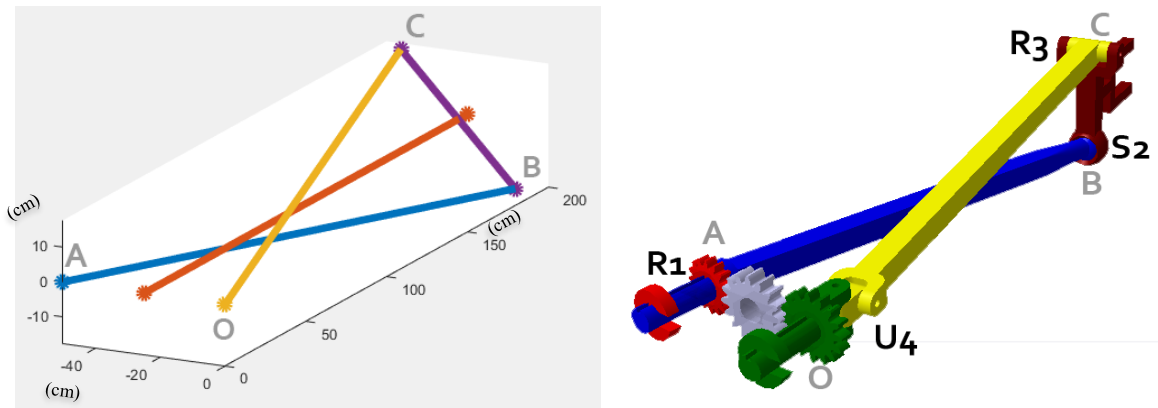


Figure 6. Matlab (left) and 3D CATIA Model (right) kinematic model. Ulna (yellow), radius (blue), wrist/hand (purple), PS-axis (red on Matlab Model)

### 3 SOLID'S SHAPE DESIGN

The parallel mechanism of the forearm has been developed for the purpose of obtaining a biofidelic design for transhumeral prostheses. Compared to the other existing solution (Herr et al., 2003) it uses a different PS axis definition that is more adapted for the design of a prosthesis. Still, both biofidelic solutions present the disadvantage of having moving parts (radius and ulna) all along the forearm. Those parts are using volume for their movement. As a consequence, it is more difficult to find the necessary space to host all of the mechatronic components, i.e. processors, batteries, and motors.

The solution found for this prosthesis design is to put some of the components directly inside those moving parts: the bones. The hand's motor is located inside the ulna, the processing components are in the radius and the remaining heavy components like motors for both pronation-supination and flexion-extension movement and battery are located in the base of the forearm (elbow (O) Figure 3) which is not moving during the pronation supination movement.

Therefore, the objective of this design research work is to define the shape of those moving parts (radius and ulna) which maximize their volume to host components while avoiding collisions. This goal is achieved using an iterative shape design algorithm.

#### 3.1 Iterative shape design algorithm

The aim of this iterative shape design algorithm is to maximize the usable volume inside the moving parts (radius and ulna). The main constraint can be translated as the solids need to complete the entire rotation, necessary for the movement around SP axis, without collisions. To achieve this, each solid is discretized into points filling the whole design space. The entire movement is then realized and a collision score discriminating the points that have been in collision with the other solids is calculated. Points with the highest scores are then removed and the procedure is repeated until no collisions can be found. More details are given in the next subsections.

##### 3.1.1 Discretization of the solids

In the context of this paper, there are two solids that need to be optimized; the radius and the ulna. Discretization of each solid has to be specified as an input to the optimization algorithm. In our case, the design space of each artificial bone is limited by the external surface of the forearm which can be approximated by a cylinder centered on the PS axis. Thus both solid are modeled by a matrix of points filling this forearm cylinder.

##### 3.1.2 Movement definition

Thanks to the kinematic model developed above, the movement is known and can be discretized. The movement studied in this optimization is the same as the one in Section 2.3 ( $\gamma_1 = \gamma_5$  with  $\gamma_1 \in [-90^\circ; 90^\circ]$  and  $p_{\gamma_1} = 1^\circ$ ). For each step, the position of the moving part is assigned to the discretized solids.

### 3.1.3 The collision score

The main constraint of the optimization is to avoid collision during the full movement while maximizing the volume of each moving solids. The collision score indicates the frequency at which each point of one solid has been in contact with the points of the other solid during the movement. As described in Section 3.1.2 this movement is discretized in  $P$  positions, for each position, the distance of the point from its closest neighbors is calculated, when it is under a certain collision threshold  $R_c$  (the point is inside the collision sphere of the other solid) the score is incremented. At the end of the  $P$  positions, the points with the highest score are removed.

### 3.1.4 Algorithm and hyper-parameters

The design algorithm repeats two step. On the first step, the collision score is computed for the entire movement (Section 3.1.3). On the second step, points that have a higher score than a specified threshold are removed. For the first iterations, the shapes are not yet optimized, as a consequence there is a large number of collisions so the threshold has to be high enough not to remove too many points. The more iterations the algorithm does, the less collisions are to be expected so the threshold needs to be adapted. For the last iteration, the threshold needs to be set to 0 so there are no collisions in the last proposed design. It is worth noting that all these thresholds are hyper parameters, and they have been optimized using a genetic algorithm.

### 3.1.5 Secondary constraints

Secondary constraints can be added if necessary. In our case, the bones cannot stand out of the forearm during the movement. Therefore, the points that are outside of the forearm cylinder defined in Section 3.1.1 during the movement are removed. To avoid complex shapes and reduce computational time, it is possible to remove manually points before the start of the iterative design process. In our study, only half the points are kept (left side for the left bone, right side for the right bone Figure 7A).

## 3.2 Results, discussion and applications

### 3.2.1 Results

The results shown in (Figure 7) are the remaining points after several iteration steps of the shape design algorithm. The colors represent the two designed solids; red for ulna and blue for radius. The number of points defining the solids shapes decrease as the algorithm iterates. The points left after the last iteration (Figure 7D) is the final result of the design algorithm. For this last shape, there is no collision between the solids during the movement.

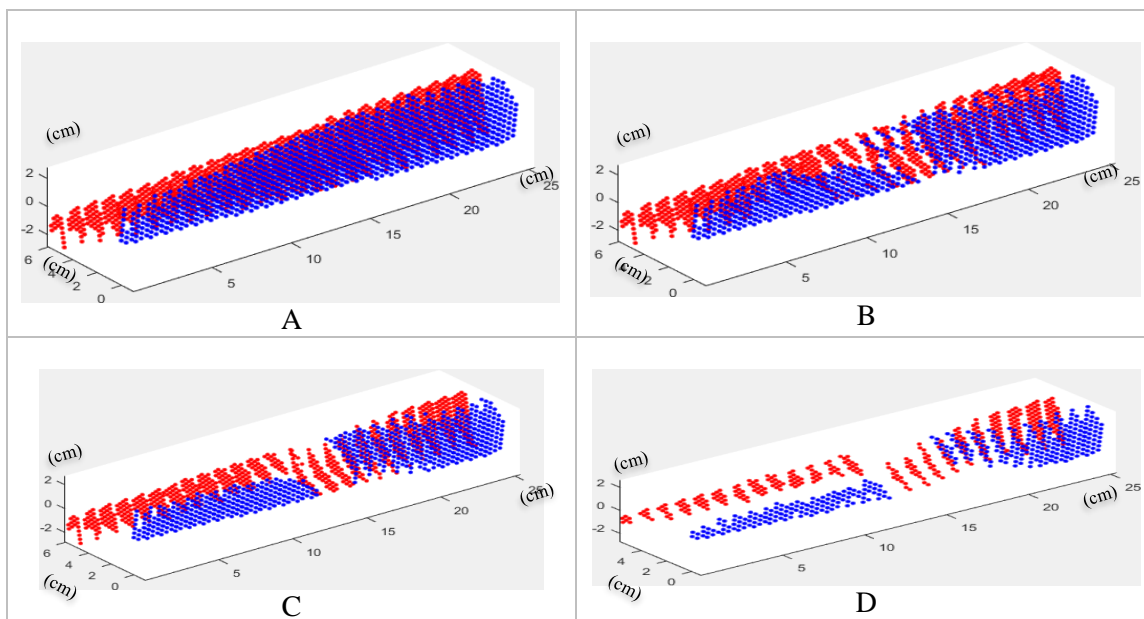


Figure 7. Algorithm iterations: (A) points kept after the 1st iteration; (B) 4th iteration; (C) 6th iteration; (D) 8th and last iteration (red ulna and blue radius)

### 3.2.2 Discussions

For the first iteration step (Figure 7A) the effect of the secondary constraints defined in Section 3.1.5 can be seen. The solids were originally basic cylinder shapes, they were then cut in half and the points out of the forearm limit cylinder during the movement were removed. For the following iteration steps (Figure 7B-C), the algorithm keeps refining the shape while the collision scores decrease.

The last iteration step (Figure 7D) shows the final shape optimized for no collision. It should be noted that the final form is not continuous so it needs to be post-processed. The proximal part is thin enough to leave space for all the components in the elbow. The distal part provides the volume necessary for the components; the hand's motor in the ulna and the processing components in the radius.

### 3.2.3 Applications

The points resulting from the iterative shape design algorithm can be used to design the part in a computer aided design (CAD) software. In our case, CATIA GSD is used to create a multi-section surface directly from the points. The empty space leaved is reconstructed while taking care to avoid collision during the pronation-supination movement (Figure 8).

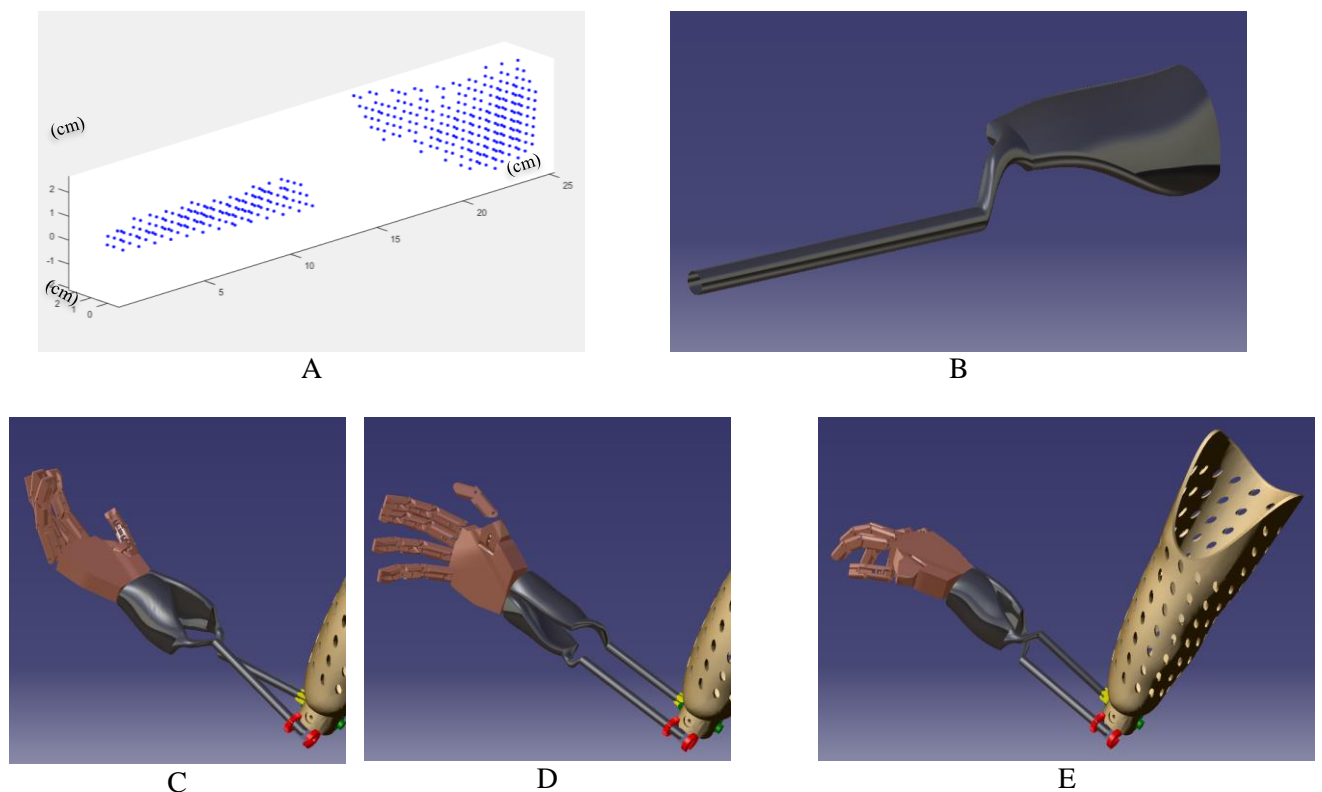


Figure 8. (A) final result of the design algorithm; (B) post-processed result; (C-D-E) pronation-supination of the designed forearm

## 4 CONCLUSION

The objective of this study was to design a biofidelic forearm with the long term aim of designing a functional prosthesis. This artificial forearm uses a parallel mechanism imitating the skeletal structure of the human forearm with the radius and the ulna. The shapes of those moving bones have been designed to allow them to host some of the prosthesis components using an original iterative shape design algorithm.

The main results are the production of a mechanism optimized to reproduce with a low and controlled error of the pronation-supination movement while using a single actuator. The mechanism solid shapes are designed to be usable in an operational prosthesis.

The resulting mechanism and solids shapes show that the biofidelic structure is a possible and feasible biofidelic alternative for prostheses.

The main perspective of this study is to prototype an operational prosthesis to show the viability of the proposed mechanism.

## REFERENCES

- Biddiss, E., Beaton, D. & Chau, T., (2007), Consumer design priorities for upper limb prosthetics.. *Disability and Rehabilitation: Assistive Technology*, 6(2), pp. 346-357.
- Cipriani, C., Zaccone, F., Micera, S. & Carrozza, M., (2008), On the shared control of an EMG-controlled prosthetic hand: analysis of user–prosthesis interaction. *IEEE Transactions on Robotics*, 1(24), pp. 170-184.
- Herr, H., Whiteley, G. & Childress, D., (2003), Cyborg Technology--Biomimetic Orthotic and Prosthetic Technology. In: S. Press, ed. Bellingham, Washington: s.n., pp. 103-143.
- Kapandji, I., (1982), *The Physiology of the Joints Volume 1 The Upper-Limb.. The Anatomy Colouring Book* 2nd Edition ed. Churchill Livingstone, London: Harper Collins.
- Laitenberger, M., Raison, M., Périé, D. & Begon, M., (2015), Refinement of the upper limb joint kinematics and dynamics using a subject-specific closed-loop forearm model. *Multibody System Dynamics*, 33(4), pp. 413-438.
- McFarlane, B., (2010), Notes on Anatomy and Physiology: The Elbow-Forearm Complex.
- Otto, I., Kon, M., Schuurman, A. & van Minnen, L., (2015), Replantation versus Prosthetic Fitting in Traumatic Arm Amputations: A Systematic Review.. *PloS one*, 10(9).
- Peerdeman, B. et al., (2011), Myoelectric forearm prostheses: State of the art from a user-centered perspective. *Journal of rehabilitation research and development*, 48(6), pp. 719-738.

## ACKNOWLEDGMENTS

We would like to thank FRQNT/INTER, NSERC and Polytechnique Montreal Foundation for their financial support for this research.